RACS Stability Analysis for VEGA FPSA Program

Federico Sciuto, Irene Cruciani**, Christophe Roux***

**AIZOON*
Palazzo Rignon - Via Po 14, 10123 Torino (Italy)
***ELV*
Corso Garibaldi 22, 00034 Colleferro (Italy)

Abstract

This paper describes the detailed stability analysis of the RACS (Roll and Attitude Control System) for VEGA launcher vehicle (LV), in the frame of the development of an Alternative Flight Program Software (FPSA). The analysis has been done with a tool that takes into account a linearized version of the actuator model and of the Pulse Width Modulation (PWM) command. The results have been validated by comparison with the practical stability margins obtained in 6DOF time domain simulations. Each RACS flight phase has a specific tuning that can be analyzed with the linear stability tool. The longer and most critical flight phases have been analyzed in this paper. The linear and practical stability margin and the phase specific Nichols plots are presented.

1. Introduction

The VEGA launcher is equipped with a RACS system in charge of controlling the roll during propelled phase and of controlling the 3 axes during ballistic phases. It allows performing the different slews and manoeuvres to accomplish the mission. The system is composed of 6 thrusters grouped into 2 clusters. The thrusters are commanded in ON / OFF thanks to a PWM command. The basically nonlinear command is approximated by a linear system in some conditions.

The propulsion system is a liquid chemical system, monopropellant (hydrazine) and blow down (pressure is not regulated but decreases in function of the consumption). This is basically a nonlinear system (thrust function of pressure and temperature, Minimum Impulse Bit…) which can be approximated by a linear system in some conditions.

The control law of the proposed Quaternion Feedback Regulator (QFR) algorithm (see Ref. [1]) is based on feedback of:

- error-quaternion (linear proportional action). It is the rotation that the LV shall perform to reach the programmed quaternion,
- error angular rate feedback (linear derivative action),
- a nonlinear body-rate term that compensates the gyroscopic coupling torque.

The desired linear dynamic behaviour is obtained by tuning the proportional and derivative gains as function of damping ratio and natural frequency of an equivalent linear second order system.

Nonlinear elements are present in the law:

- thresholds on attitude error,
- thresholds on angular rate,
- minimum activation duration.

In the literature, several approaches are found to deal with such system. Several are basically nonlinear (limit cycles analysis), others use describing function method [6], some authors propose analytical formula to treat the PWM [6],[4]. In some articles ([2], [3], [5]) , a space state approximated representation of the PWM is proposed we will use.

The approach presented in this article is fundamentally linear with two aspects: linearization of PWM and of RACS actuator system.

The stability is analysed for each tuning computed for each flight phase. The tunings are made generic thanks to a scaling of the gains adapted to full inertia matrix of the launcher. The launcher inertia varies mission to mission in function of the payload characteristics.

The topics presented in this paper are:

- RACS model and its linearization description;
- Linear and practical stability results
- Results comparison.

2. Linearized RACS model

2.1 RACS model

For each thruster, the mathematical model involves the thrust level *F*, the mass flow rate *m'*, the temperature of the chamber *Tc* and the pressure *pfeed*. It is a differential system with two modes of functioning (ON and OFF):

Opened Valve (ON mode):

$$\begin{cases} \dot{T}_C = c_1 \; p_{feed}^{\;c_2} \left(T_{C,\max} - T_C\right) \\ c_3 T_C \dot{F} = c_6 \; p_{feed}^{\;c_7} \; T_C^{\;2} - c_8 \; F \; T_C^{\;3/2} \\ \dot{m} = c_{11} \; p_{feed}^{\;c_{12}} \end{cases} \qquad \textbf{(1)}$$

$$T_{C,\max} = c_9 \; p_{feed}^{\;c_{10}}$$

Closed Valve (OFF mode):

$$\begin{cases} \dot{T}_C = -c_{13} \left(T_C - T_{environment}\right) \\ \dot{F} = -F \left[1 + \Omega\left(t - t_{OFF} - \Delta t_{DELAY\_OFF}\right)\right]^{c_{18}\,\Omega} \\ \dot{m} = 0 \end{cases} \qquad \textbf{(2)}$$

2.2 RACS linear continuous-time system

The complete linear continuous-time model used for the stability analysis is reported hereafter.

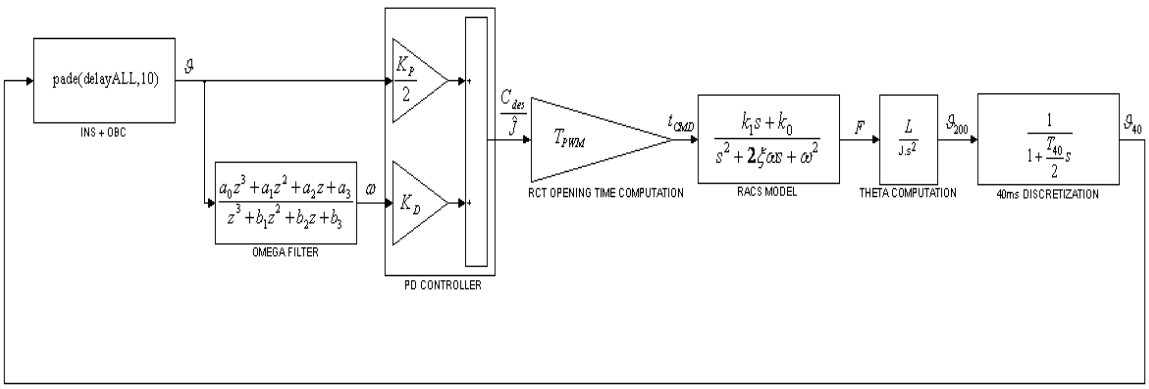

Figure 1: RACS linear continuous-time model

From left to right, we first have the INS and OBC system that in this linearization are considered as pure delays. The other delay of that model is that introduced by the actuators. The total delay is represented for state space analysis by a Padé approximation of order 10.

The next block is the PD control law:

$$\frac{C_{des}}{\hat{J}} = \frac{K_P}{2}\vartheta + K_D\omega \qquad \textbf{(3)}$$

The gains K_P and K_D are the proportional and derivative (PD) gains respectively. The signal out of the PD has the dimension of a desired couple divided by the estimated inertia $C_{des}/\hat{J}$.

The angular rate ω is computed as the derivative of the angle ϑ by the means of the following discrete filter:

$$\frac{a_0 z^3 + a_1 z^2 + a_2 z + a_3}{z^3 + b_1 z^2 + b_2 z + b_3}$$

The following gain block makes explicit the calculation of the commanded time (t_{CMD}), according to the following equation.

$$\frac{t_{CMD}}{T_{PWM}} = \frac{C_{des}}{\hat{F}\hat{L}} \qquad \textbf{(4)}$$

Where

T_{PWM} is the modulation sampling time

$\hat{F}\hat{L}$ is the estimated torque given by the RACS

$\hat{F}$ is the estimated thrust given by the RACS

$\hat{L}$ is the estimated torque arm

The RCT thrust estimation is a polynomial function of the residual mass estimation $\bar{m}$:

$$\hat{F} = d_0 + d_1\bar{m} + d_2\bar{m}^2 + d_3\bar{m}^3 \qquad \textbf{(5)}$$

Equation **(4)** is derived from the equality between desired and estimated impulse

$$\hat{J}\left(\frac{K_P}{2}\vartheta + K_D\omega\right)\cdot T_{PWM} = \hat{F}\cdot\hat{L}\cdot t_{CMD} \qquad \textbf{(6)}$$

The following block represents the Reaction Control Thruster (RCT) model. This model is represented by the means of a second order transfer function as explained in §2.6. The real torque is obtained from the thrust by multiplication by the real lever arm L. The angular acceleration is deduced from the torque by division by the launcher inertia.
The sampling process at T_{40} = 40 ms is simplified by the transfer function:

$$\frac{1}{1+\frac{T_{40}}{2}s} \qquad \textbf{(7)}$$

From this, we obtain the open-loop transfer function:

$$sys = \text{pade(delayALL,10)}*\left(\frac{K_P}{2}\vartheta + K_D\omega\right)*T_{PWM}\,\frac{\hat{J}}{\hat{F}\hat{L}}*\frac{a_1 s + a_0}{s^2 + 2\xi\omega s + \omega^2}*\frac{L}{Js^2}*\frac{1}{1+\frac{T_{40}}{2}s} \qquad \textbf{(8)}$$

In stability analysis, variations in the moment arms are neglected, so that we have $\hat{L} = L$ and our final equation is:

$$sys = \text{pade(delayALL,10)} * \left(\frac{K_P}{2} \vartheta + K_D \omega \right) * T_{PWM} \frac{\hat{J}}{\hat{F}} * \frac{a_1 s + a_0}{s^2 + 2\xi\omega s + \omega^2} * \frac{1}{Js^2} * \frac{1}{1 + \frac{T_{40}}{2} s} \quad \textbf{(9)}$$

This is the linear and continuous-time part of the system. The other element of the control loop is the Pulse Width Modulation (PWM) which is essentially nonlinear. A linear representation of this PWM element is explained in section §2.5.

2.3 RACS generic tuning

The independence of the closed loop dynamic behaviour from the LV inertia is guaranteed by a generic characterization of the control gains, valid and applicable for all mission types. From equation **(6)** the desired couple is obtained through the LV inertia.

The desired closed loop behaviour is obtained by tuning the proportional and derivative gain as function of damping ratio and natural frequency of an equivalent linear second order system. It is obtained as follows:

if λ is a unit vector along the eigenaxis, the vector part of the quaternion can be written as $q = \sin(\vartheta)\lambda$, where ϑ is the rotation angle. Assuming that the angular velocity is about equal to $\dot{\vartheta}\lambda$, the characteristic equation of the closed loop system becomes:

$$\left(\ddot{\vartheta} + K_D \dot{\vartheta} + K_P \sin\left(\frac{\vartheta}{2} \right) \right) \hat{J}\lambda = 0 \quad \textbf{(10)}$$

For gain tuning, it is approximated by $\sin(\vartheta/2)$ by $\vartheta/2$. So if $\hat{J}\lambda \neq 0$, we obtain a linear second-order equation:

$$\ddot{\vartheta} + K_D \dot{\vartheta} + K_P \frac{\vartheta}{2} = 0 \quad \textbf{(11)}$$

where the damping ratio ζ and the natural frequency ω_n, that are independent from the Inertia Matrix, satisfy :

$$K_D = 2\zeta\omega_n; \qquad K_P / 2 = \omega_n^2$$

2.4 RACS non linearity

The RACS non-linearity that has not be represented in the linearization is the dead-band, that is the $\vartheta - \omega$ band within no command is requested by the algorithm. This band depends on the PD controller gain and on t_{MIN} .

t_{MIN} is a tuning parameter, it is the minimum t_{CMD} after that a Minimum Impulse Bit (MIB) is commanded.

From equation **(6)** changing t_{CMD} with t_{MIN} the following formula is obtained:

$$\omega_0 = \frac{\hat{F} \cdot \hat{L} \cdot t_{MIN}}{K_D \cdot \hat{J} \cdot T_{PWM}} \quad \textbf{(12)}$$

The ω given by a MIB is:

$$\omega_{MIB} = \int_0^{t_{MIB}} \frac{F \cdot L}{J} = \frac{F \cdot L \cdot t_{MIB}}{J} \quad \textbf{(13)}$$

In order to avoid a non-linear effect (a high frequency oscillation called chattering) caused when the dead-band is narrower than the minimum $\Delta\omega$ given by a MIB it is mandatory to maintain the constraint:

$$\omega_{MIB} < 2\omega_0 \quad \rightarrow \quad \frac{F \cdot L \cdot t_{MIB}}{J} < 2\frac{\hat{F} \cdot \hat{L} \cdot t_{MIN}}{K_D \cdot \hat{J} \cdot T_{PWM}} \qquad \textbf{(14)}$$

So in nominal case where the estimation is equal to the reality, the following relation is obtained:

$$K_D < 2\frac{t_{MIN}}{t_{MIB} \cdot T_{PWM}}$$

2.5 General derivation of the PWM linear SISO model

The purpose here is to represent the linear behaviour of the compound system conformed by PWM and the plant downstream of it. Starting with the continuous-time representation of the plant, the input is modified as expected from the PWM in order to justify an approximation that leads to the PWM-plant representation we are looking for (for a more detailed explanation see Ref. [2]).

Consider a generic "original" linear system, the response of which can be written in the well-known form:

$$x(t) = e^{A(t-t_0)}x(t_0) + \int_{t_0}^{t} e^{A(t-t')}Bu(t')dt' \qquad \textbf{(15)}$$

PWM means that over each successive interval of time of length T, the command $u(t)$ is converted in a pulse of constant height H and width τ such that the following applies:

$$\int_{t_0}^{t_0+T} u(t')dt' = \int_{t_0}^{t_0+\tau} Hdt' + \int_{t_0+\tau}^{t_0+T} 0dt' = H\tau \qquad \textbf{(16)}$$

If $u(t)$ is a force, **(16)** indicates that PWM is such that the total impulse (force per time) given as an input is unvaried.

We might explicitly express τ it as a function of discrete time instants as $\tau = \tau(kT)$. Actually in our real RACS, τ is not estimated as

$\tau(kT) = \dfrac{\int_{kT}^{kT+T} u(t')dt'}{H}$ but as $\tau(kT) = u(kT)\dfrac{T}{H}$.

This implies that $u(t)$ is sampled at a period T.

Inside an interval $[kT, (k+1)T]$, Eq. **(15)** can therefore be rewritten as:

$$\begin{aligned} x(kT+T) &= e^{AT}x(kT) + \int_{kT}^{kT+T} e^{A(kT+T-t')}Bu(t')dt' \\ &= e^{AT}x(kT) + \int_{kT}^{kT+\tau} e^{A(kT+T-t')}BHdt' \end{aligned} \qquad \textbf{(17)}$$

Now a fundamental approximation is made by considering $e^{A(kT+T-t')}$ constant and equal to e^{AT} inside the interval $[kT, kT+\tau]$. This allows to write the response as:

$$x(kT+T) = e^{ATx(kT)} + e^{AT}BH\tau(kT) \qquad \textbf{(18)}$$

This approximation is better for smaller τ and arguably applies for the RACS system object of this document, for which $T = 200ms$ and the minimum possible impulse width is $\tau = 20ms$.

Putting $A_M = e^{AT}$ and $B_M = e^{AT} BHT$ we have:

$$x(kT+T) = A_M x(kT) + B_M \frac{\tau(kT)}{T} \qquad \textbf{(19)}$$

which formally has the form of the state-space representation of a discrete-time linear system.

$\tau(kT)/T$ is universally known as duty cycle.

We call this last system the "PWM system". For our RACS system, the quantity $H\tau$ represent an impulse bit, abbreviated Ibit.

The eigenvalues of the original system, s_i, are the continuous-time equivalent of the eigenvalues of the PWM system z_i, as they verify the sampling transformation $z_i = e^{s_i T}$. However, the two systems have different input matrices, which entails different Nichols plots and therefore different robustness properties.

2.6 RACS linear transfer function derivation

In order to fit the non-linear RACS model presented in §2.1, a transfer function for each working condition has been chosen.

As it is possible to see in equation **(1)** and **(2)** the RACS output depends strongly on the opening time, the operative temperature and the operative pressure, so it was necessary to find a transfer function for each working condition. For what concerns temperature only the boundary conditions have been taken into account. For the pressure five different conditions have been chosen. We have selected the opening time related to the minimum impulse bit (MIB), that is the RACS impulse related to the minimum commanded opening time.

In the following figures the example of the output variability with the operative conditions:

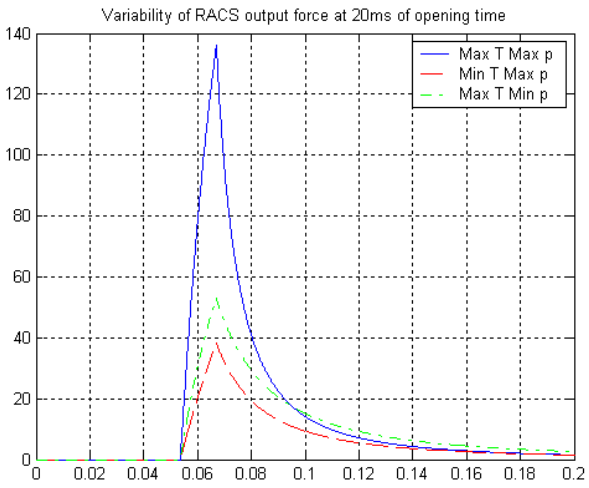

Figure 2: RACS force variability at 20ms opening time

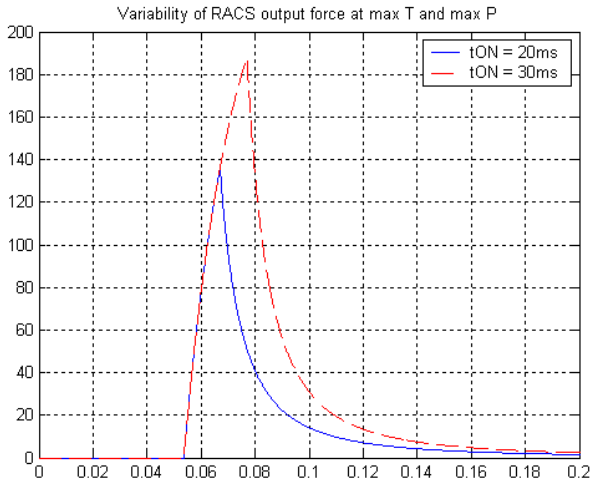

Figure 3: RACS force variability with opening time

The RACS conditions selected are:

- opening times t_{cmd}: 20ms (MIB) and 30ms
- temperatures: 289K and 1223K
- pressures: 8bar, 12bar, 18bar, 24.7bar and 26bar

In order to find an equivalent transfer function (TF) for the RACS model, an optimization model has been used:

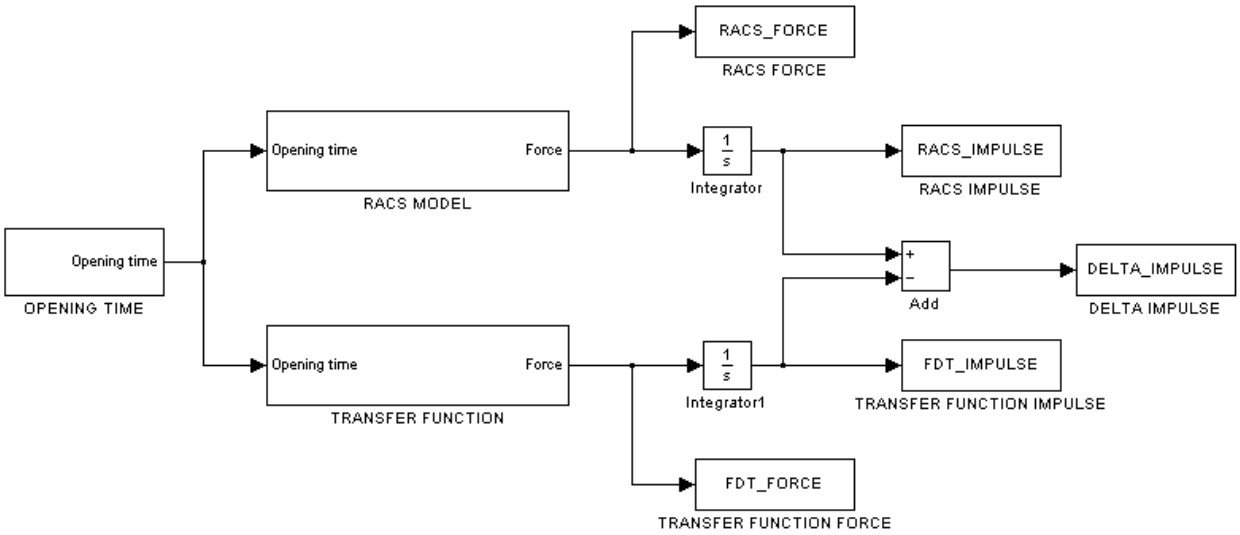

Figure 4: TF finder Simulink Model

In this paragraph the TF output are compared with the RACS model output in nominal and scattered conditions (Max and Min Impulse). The TF found represent the RCT thrust and they are tuned in order to fit the impulse and the centroid time of the RACS model.
The TF structure is:

$$\frac{k_1 s + k_0}{s^2 + 2\xi\omega s + \omega^2} \qquad \textbf{(20)}$$

From equation **(9)** the RACS model parameters affected by uncertainty are:

t_{CMD} that depends on the time delay in opening and closing actuators valves,

J that depends on the construction of the LV,

F that is strictly linked to the RACS propellant mass m that depends on the RACS tank loading process

The scattering considered are taken as the maximum value specified in the Launcher avionics specification.

The Max Impulse conditions for RACS model are obtained with max J, min m and max t_{CMD}.

The Min conditions for RACS model are obtained with min J, max m and min t_{CMD}.

The scattering on t_{CMD} and m can't be represented in the TF, so these scattering will be represented only with a scattering percentage on the TF output tuned for each working condition.

The Max Impulse condition for TF for what concerns the two previous scattering considered is obtained with Force scattering = +F_Max%;

The Min Impulse conditions for TF is obtained with Force scattering = -F_Min%;

F_Max and F_Min are working condition dependant

Hereafter a subset of the working condition considered are:

Table 1: RACS working conditions description

	Opening time [ms]	Operative temperature [K]	Operative pressure [bar]
Case 1	20	1223	26
Case 2	20	289	8
Case 3	30	1223	26
Case 4	30	289	8

For each working condition, a different TF has been found:

Table 2: RACS working conditions TF definition

	a_0	a_1	ω	ξ	F_Max [%]	F_Min [%]
Case 1	231200	16000	31.4159	1.63	53.9	51.1
Case 2	87630	1400	31.4159	2.02	48.5	48.8
Case 3	235440	17000	31.4159	1.61	32.5	30.4
Case 4	83100	1600	31.4159	1.99	28.7	28.0

Following an example of TF (Case 1):

- t_opening = 20ms;
- Temperature = 1223K;
- Pressure = 26bar.

In this case the TF coefficients are $a_0 = 231200$ $a_1 = 16000$ $\omega = 31.4159$ $\xi = 1.63$

The scattering on output found are:

F_Max = 53.9%;
F_Min = 51.1%;

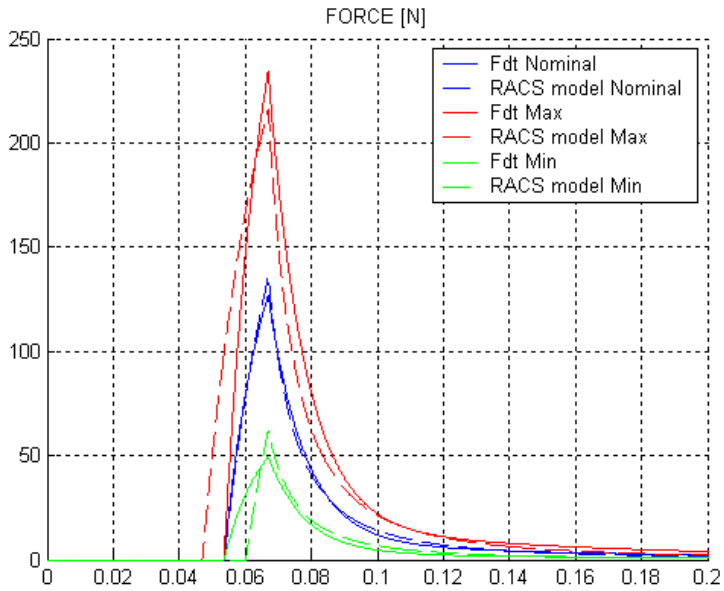

Figure 5: RCT thrust comparison

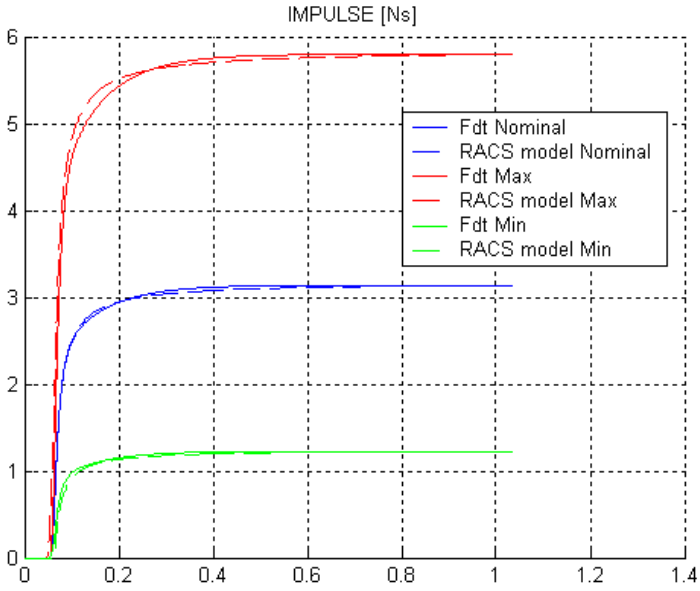

Figure 6: RCT impulse comparison

Table 3: Impulse and centroid time comparison

	RACS model			TF		
	Max	**Nom**	**Min**	**Max**	**Nom**	**Min**
Impulse 20/180 [Ns]	5.5786	2.9916	1.1554	5.5475	3.0038	1.1751
Centroid time 20/180 [ms]	77.8	82.9	88.5	84.2	84.2	84.2
Impulse 20/1000 [Ns]	5.7975	3.1396	1.228	5.7971	3.139	1.228
Centroid time 20/1000 [ms]	91.2	99.4	108.9	94.8	94.8	94.8
Impulse 20/10000 [Ns]	5.8431	3.1705	1.2432	5.7971	3.139	1.228
Centroid time 20/10000 [ms]	110.7	123.7	139.2	94.8	94.8	94.8

3. Stability results

In order to obtain the practical stability margins 6dof simulations have been performed increasing the RACS commands delay for delay margins and increasing the RCTs thrust for gain margin.

This results have been obtained with nominal simulations with the following conditions:

- No noise
- No Sloshing

The sloshing model has been disabled in order to have a better correspondence with the stability tool results that doesn't include the sloshing model. For each phase are reported the 6DOF result and the nominal, maximum and minimum results of the tool. As maximum and minimum results, the maximum and minimum margin obtained by the full analysis are taken into account. The full analysis considers all the transfer function and the maximum and minimum impulse scattering. The nominal result considers only the nominal working condition of the analyzed phase and it will be reported for each phase.

The flight phase chosen is the 3-axis PL release. The tuning in this phases is:

Table 4: Tuning of 3-axis PL release phase

	KD		KP	
PL 3-axis release	**x-axis**	**y/z-axis**	**x-axis**	**y/z-axis**
	2.0	2.0	3.0	3.0

3.1 Linear stability results

The nominal working condition for this phase is the following one:

- t_opening = 20ms;
- Temperature = 1223K;
- Pressure = 18bar.

The relative TF is:

Table 5: RCT transfer function coefficient

a_0	a_1	ω	ξ
207800	12000	31.4159	1.58

The TF characteristics are:

Table 6: Impulse and centroid time comparison

	RACS model			TF		
	Max	**Nom**	**Min**	**Max**	**Nom**	**Min**
Impulse 20/180 [Ns]	4.8391	2.6366	1.0508	4.8236	2.6638	1.0804
Centroid time 20/180 [ms]	82.1	87.6	93.4	89.9	89.9	89.9

The boundary conditions are the following ones:

Max Delay & Gain	Min Delay & Gain
• t_opening = 30ms;	t_opening = 20ms;
• Temperature = 289K;	Temperature = 1223K;
• Pressure = 24.7bar.	Pressure = 12bar.

The relative TF are:

Table 7: RCT Max Delay and Gain transfer function coefficient

a_0	a_1	ω	ξ
108700	4750	31.4159	1.6

Table 8: RCT Min Delay and Gain transfer function coefficient

a_0	a_1	ω	ξ
188240	9000	31.4159	1.61

The TF characteristics are:

Table 9: Impulse and centroid time comparison of Max Delay and Gain

	RACS model			TF		
	Max	**Nom**	**Min**	**Max**	**Nom**	**Min**
Impulse 30/170 [Ns]	3.6905	2.3098	1.2781	3.6985	2.3474	1.3202
Centroid time 30/170 [ms]	95.6	100.1	104.7	103.4	103.4	103.4

Table 10: Impulse and centroid time comparison of Min Delay and Gain

	RACS model			TF		
	Max	**Nom**	**Min**	**Max**	**Nom**	**Min**
Impulse 20/180 [Ns]	4.1965	2.3210	0.9450	4.1795	2.3549	0.9815
Centroid time 20/180 [ms]	87.2	93.2	99.5	96.7	96.7	96.7

The results are:

Table 11: Delay margins of linear stability analysis

		Nominal delay margin [ms]	**Maximum delay margin [ms]**	**Minimum delay margin [ms]**
PL release 3-axis	x-axis	343.25	680.11	261.03
	y/z-axis	343.25	680.11	261.03

Table 12: Gain margins of linear stability analysis

		Nominal gain margin [dB]	**Maximum gain margin [dB]**	**Minimum gain margin [dB]**
PL release 3-axis	x-axis	14.7967	21.276	12.1385
	y/z-axis	14.7967	21.276	12.1385

Nichols plots:

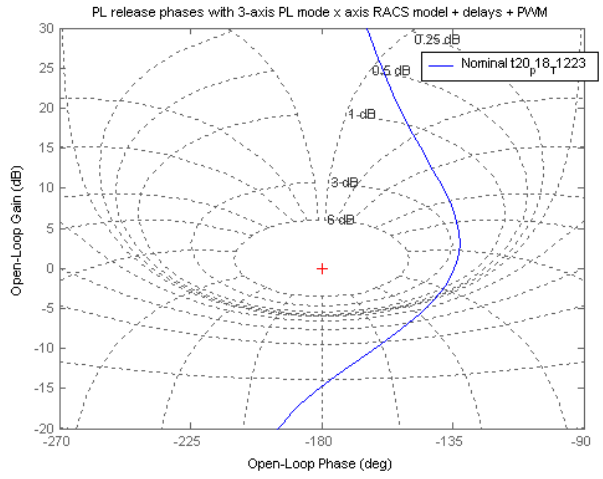

Figure 7: RACS commands

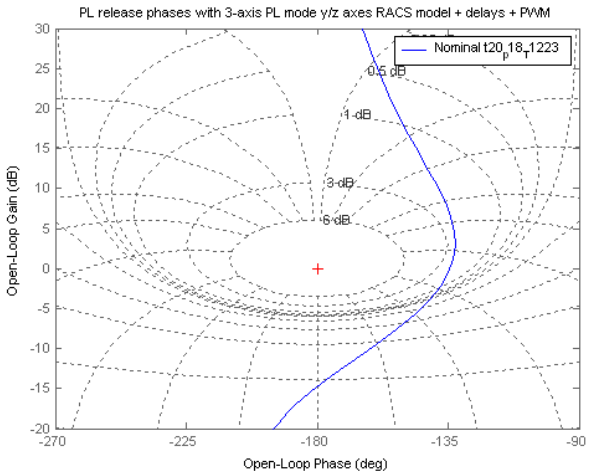

Figure 8: LV angular rates in body RF

3.2 Practical stability results

In order to find the practical stability margins, 6dof simulations have been performed increasing the RACS commands delay for delay margins and increasing the RCTs thrust for gain margin. The practical stability analysis has been performed decoupling the delay and gain effect.

From the following plots it is possible to see that increasing the command delay till 0.7s the LV behaviour remains stable:

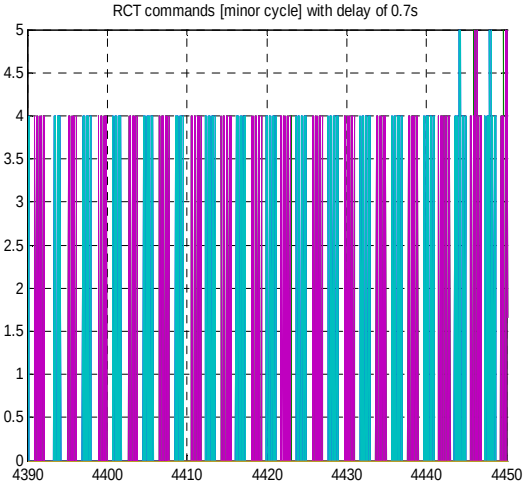

Figure 9: RACS commands

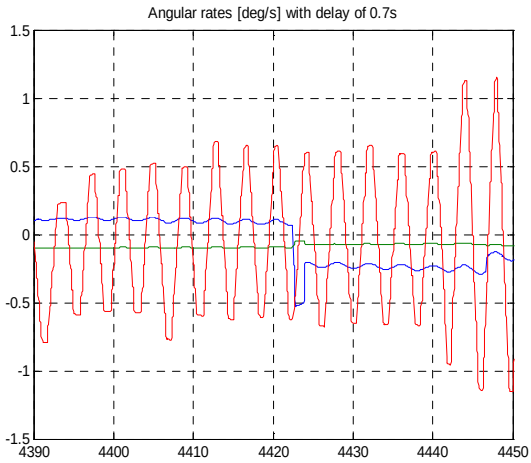

Figure 10: LV angular rates in body RF

Instead increasing the command delay to 0.75s it is possible to see that the LV starts to diverge:

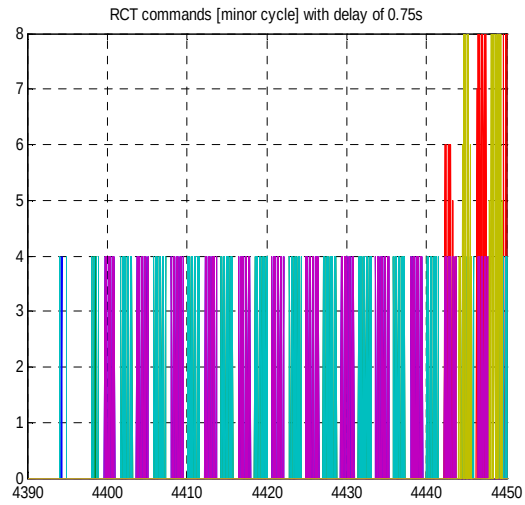

Figure 11: RACS commands

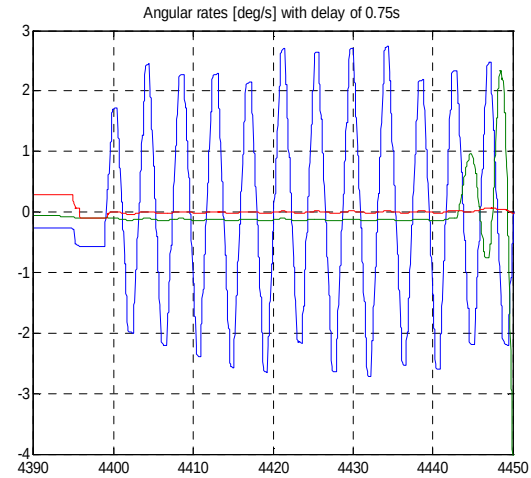

Figure 12: LV angular rates in body RF

From the following plots it is possible to see that increasing the thrust gain till 15.5dB the LV behaviour remains stable:

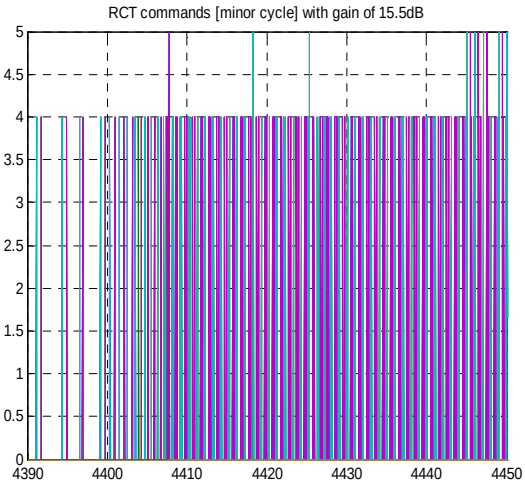

Figure 13: RACS commands

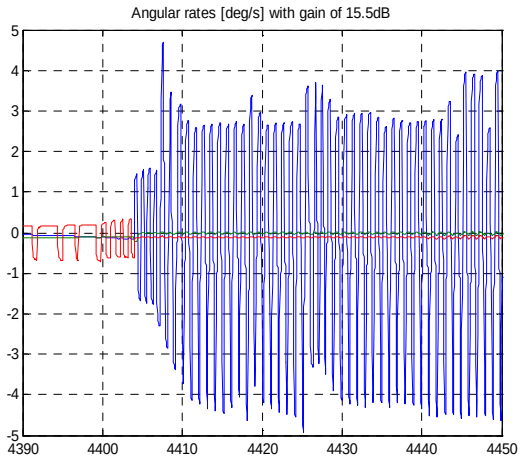

Figure 14: LV angular rates in body RF

Instead increasing the thrust gain to 16dB it is possible to see that the LV starts to diverge:

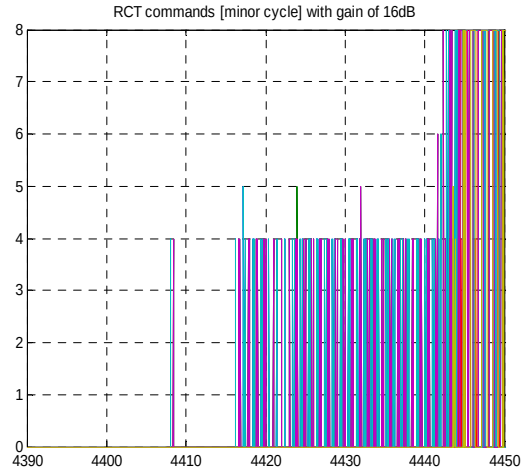

Figure 15: RACS commands

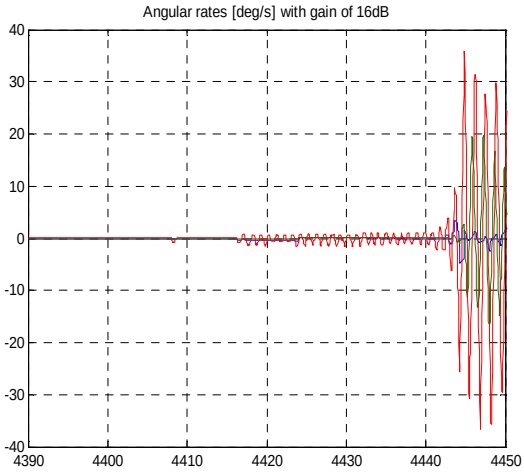

Figure 16: LV angular rates in body RF

The results are:

Table 13: Delay margins of practical stability analysis

		Noiminal delay margin [ms]
PL release 3-axis	x-axis	>700
	y/z-axis	>700

Table 14: Gain margins of practical stability analysis

		Noiminal gain margin [dB]
PL release 3-axis	x-axis	>15.5
	y/z-axis	>15.5

4. Conclusion

A method to analyse VEGA RACS control system based on the

- linearization of PWM system (approximated state space representation)
- linearization of the actuator system (approximated by transfer functions in different set points),

has been presented.

Classical methods based on SISO model are used (Nichols plots, poles…). The approach has been validated by comparison with simulations on full 6DOF model. The advantage of the stability analysis is to be aware of the margins at the very beginning of the design phase and to not discover problems (instability or chattering) at the moment of the simulations campaigns based on Monte-Carlo.

The results obtained for the selected phase are:

Delay margin

Table 15: Delay margins comparison

	Time domain delay margin [ms]	**Frequency domain delay margin [ms] at 18bar**	**Delta [ms]**
x-axis	700	343.25	356.75
y/z-axis	700	343.25	356.75

Gain margin

Table 16: Gain margins comparison

	Time domain gain margin [dB]	**Frequency domain gain margin [dB] at 18bar**	**Delta [dB]**
x-axis	15.5	14.7967	0.7033
y/z-axis	15.5	14.7967	0.7033

The big difference seen in delay margin is simply explained by the big variability of the centroid time with the RACS condition that are not constant in time domain. On the opposite, the impulse bit has little variation with the RACS condition. In conclusion both delay and gain margin the frequency domain results are more conservative than the time domain ones. So it is possible to affirm that the results obtained by the frequency domain analysis can be used in order to verify the RACS stability requirement.

References

[1] Cuciniello, G., I. Cruciani, F. Nebula, F. Sciuto, F. Corraro and M. Cicala. 2012. RACS QFR ALGORITHM FOR VEGA FPSA PROGRAM. In: *63rd IAC, Naples, Italy*.

[2] Bernelli-Zazzera F. and P. Mantegazza. 1992. Pulse-Width Equivalent to Pulse-Amplitude Discrete Control of Linear Systems. *Journal of Guidance, Control, and Dynamics*, Vol. 15, No. 2.

[3] Bernelli-Zazzera F., Mantegazza P. and V. Nurzia. 1998. Multi-Pulse-Width Modulated Control of Linear Systems. *Journal of Guidance, Control, and Dynamics*, Vol. 21, No. 1.

[4] Anthony T.C., Bong Wie and S. Carroll. 1990. Pulse Modulated Control Synthesis for a Flexible Spacecraft. *Journal of Guidance, Control, and Dynamics*, Vol. 13, No. 6.

[5] Ieko T., Ochi Y. and K. Kanai. 1999. New Design Method for Pulse-Width Modulation Control Systems via Digital Redesign. *Journal of Guidance, Control, and Dynamics*, Vol. 22, No. 1.

[6] Bong Wie. 1998. Space Vehicle Dynamics and Control. AIAA Education Series